Nerve Regeneration in *Caenorhabditis elegans* After Femtosecond Laser Axotomy

Mehmet Fatih Yanik, Hulusi Cinar, Hediye Nese Cinar, Aaron Gibby, Andrew D. Chisholm, Yishi Jin, and Adela Ben-Yakar

(Invited Paper)

***Abstract*—We perform submicrometer-scale surgery with femtosecond lasers to study nerve regeneration in the tiny nematode *Caenorhabditis elegans*, an invertebrate model organism with only 302 neurons. By cutting nanoscale nerve connections inside the nematode *C. elegans*, the feedback loops that control backward motion of the worm can be disconnected. This operation stops the whole worm from moving backward while leaving its forward motion intact. The femtosecond laser-based axotomy creates little peripheral damage so that the cut axons can regrow, and the worms recover and move backward again within one day. We conduct several assays to assess target specificity, damage threshold, and the extent of femtosecond laser axotomy. We also study nerve regeneration in touch neurons, and report an interesting type of nerve regeneration that salvages the severed parts of neurons from degeneration. The use of femtosecond laser pulses as a precise surgical tool allowed, for the first time, observation and study of nerve regeneration in *C. elegans* with a simple nervous system. The ability to perform precise axotomy on such organisms provides tremendous research potential for the rapid screening of drugs and for the discovery of new biomolecules affecting regeneration and development.**

***Index Terms*—Laser ablation, microscopy, nervous system, nonlinear optics, plasma generation, pulsed lasers, surgery.**

I. Introduction

UNDERSTANDING the biological basis of nerve regeneration is an important step towards development of novel therapies for human neurological diseases [1]. *In vivo* studies of nerve regeneration have been limited to complex vertebrate model organisms such as mouse and zebrafish [2] due to lack of precise techniques for severing axons (axotomy). The study of nerve regeneration in simpler invertebrate model organisms can promise tremendous potential due to powerful and rapid screening techniques. Using femtosecond laser surgery, we recently demonstrated the feasibility of precision axotomy in a simple organism *Caenorhabditis elegans*, having only 302 neurons, and observed functional regeneration of operated axons following surgery [3]. This precise surgical technique opens the experimental access to study nerve regeneration *in vivo* in an organism with a simple nervous system, for the first time.

After a brief introduction to femtosecond laser surgery in Section II, we describe our experimental setup in Section III. In Section IV, we study the pulse energy threshold for transition from photobleaching to photodamage regime by time-lapse green fluorescent protein (GFP) fluorescence imaging, photobleaching, and recovery experiments. In Section V, we study femtosecond laser axotomy process by dye-filling experiments to confirm axotomy, target specificity, and damage extent. In Section VI, we describe our studies on nerve regeneration in motor neurons. Sections VI-A and VI-B cover our morphological and behavioral studies, respectively. In Section VII, we study nerve regeneration in another type of neurons called the touch neurons, and report an interesting nerve regeneration phenomenon in *C. elegans*, which salvages the severed parts of neurons from degeneration.

II. Laser Surgery With Near-Infrared (NIR) Femtosecond Pulses

Laser-induced ablation and surgery with continuous UV irradiation has been successfully used in cell biology [4]–[8] and in studies of morphogenesis in small organisms [9]. However, with nanosecond or longer duration laser pulses, high energies (0.5 μJ [10]) are required for initiation of laser ablation, which can lead to significant collateral damage [11]. Furthermore, the use of UV light leads to out-of-focus absorption and low penetration depth because of the strong absorption of UV radiation by the tissue environment. Recently, there has been a growing interest in the use of ultrashort NIR laser pulses in laser surgery [12]. In particular, due to increased peak intensities and efficient plasma generation with femtosecond pulses [11], [13], [14], pulse energies as low as a few nano-Joules were shown to be sufficient for controlled laser ablation of subcellular structures [15]–[20]. At such low energies, *in vitro* chromosome dissection with subdiffraction resolution has been achieved [21] because of the strong nonlinear dependence of the ablation process to the photon intensity, and reduced collateral effects. Ultrashort NIR laser pulses have also been used in efficient DNA transfection [22], in study of morphogenesis during development [23],

Manuscript received December 12, 2005; revised May 22, 2006.

M. F. Yanik is with the Department of Electrical Engineering, Massachusetts Institute of Technology, Cambridge, MA 02139 USA, and also with Ginzton Laboratory, Stanford University, Stanford, CA 94305 USA (e-mail: yanik@mit.edu).

H. Cinar, H. N. Cinar, and A. D. Chisholm are with the Department of Molecular Cell and Developmental Biology, Sinsheimer Laboratories, University of California, Santa Cruz, CA 95064 USA.

A. Gibby is with the Ginzton Laboratory, Stanford University, Stanford, CA 94305 USA.

Y. Jin is with the Department of Molecular Cell and Developmental Biology, Sinsheimer Laboratories, University of California, Santa Cruz, CA 95064 USA, and also with the Howard Hughes Medical Institute, Chevy Chase, MD 20815-6789 USA.

A. Ben-Yakar was with the Ginzton Laboratory, Stanford University, Stanford, CA 94305 USA. She is now with the Department of Mechanical Engineering, University of Texas at Austin, Austin, TX 78712 USA.

Digital Object Identifier 10.1109/JSTQE.2006.879579

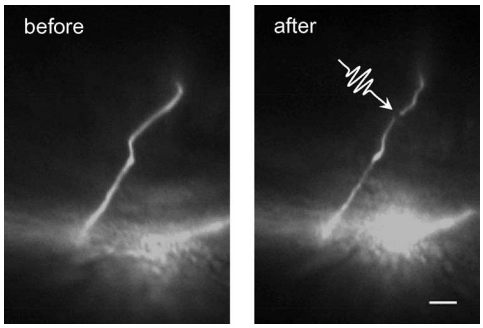

Fig. 1. Example of femtosecond laser axotomy with 10-nJ pulse energy (200-fs duration, 400 pulses at the rate of 1 kHz). Fluorescence images of an unc-25::GFP-labeled D-neuron axon before and 10 min after axotomy. The second image shows a photodisrupted region with 1.2-μm length. This indicates that an axon volume of a few femtoliters is ablated at the focal point. Assuming an axon diameter of 0.3 μm, we estimate that the ablated volume of the axon is less than 0.1 fL [1.2 μm $\times\pi$ (0.15 μm)^2]. Scale bar is 5 μm. The ventral part of the worm is toward the bottom of the image.

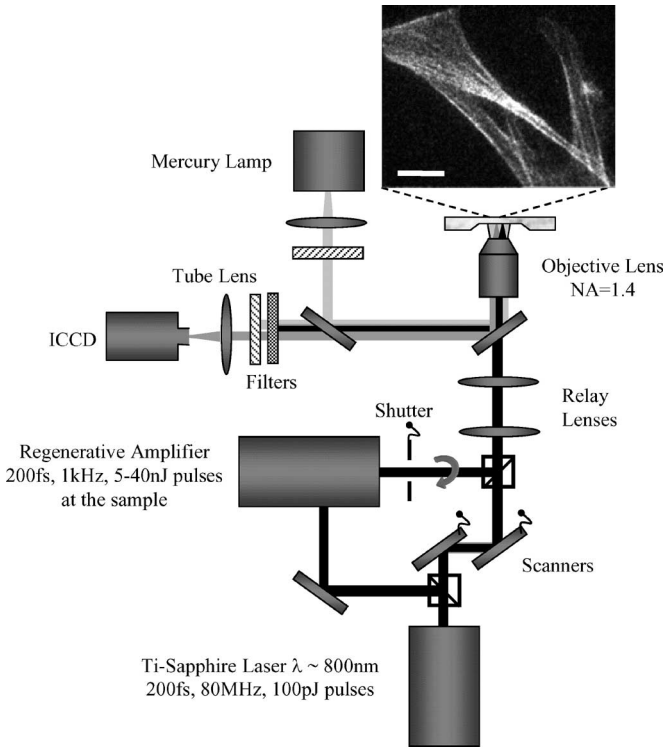

Fig. 2. Experimental setup for femtosecond laser nanosurgery with simultaneous two-photon imaging capability. The inset shows a two-photon image of F-actin filaments labeled with Alexa Fluor 488 dye. Scale bar is 5 μm. The image is taken by an ICCD camera instead of a photomultiplier.

and in targeted injury of blood vessels [24]. At lower pulse energies, NIR femtosecond laser pulses also allow two-photon imaging of multicellular organisms with deep penetration depth and long imaging times [25].

Recently, for axotomy of subcellular neuronal processes *in vivo*, we have performed femtosecond laser nanosurgery using a homemade microscope with two-photon imaging capability [3]. We succeeded in rapidly cutting single axons inside *C. elegans* with pulse energies of 10–40 nJ at the specimen, using only 100 tightly focused 200-fs short (before optical setup) near infrared laser pulses. This resulted in the vaporization of axon volumes of about 0.1–0.3 fL, assuming an average axon diameter of 0.3 μm (Fig. 1). To initiate femtosecond laser ablation, the laser fluence (energy per unit area) has to exceed a certain threshold. The minimum fluence (2.2 ± 0.2 J/cm^2 corresponding to 10-nJ pulse energy) used in our studies is close to the measured optical breakdown thresholds of 1–2 J/cm^2 in transparent dielectric materials such as water [11], [13], [14]. Close to the threshold fluences, mechanical effects due to plasma expansion and shockwaves are expected to be significantly reduced [14] with respect to other laser surgery techniques that require much higher energies (e.g., 0.4 μJ with 0.5-ns pulses [26]). Furthermore, the use of low repetition rate pulses (1 kHz, 10-μW average power) reduces heat accumulation and the resulting thermal damage to the environment. We were able to cut individual nerve processes without damaging other processes within a few micrometers proximity (Section V).

III. Optical Setup

A tunable Ti-Sapphire mode-locked laser (Coherent, "Mira 900") produces 200-fs short pulses with a repetition rate of 76 MHz and an energy of 5 nJ (Fig. 2). For axotomy, a regenerative amplifier (Positive Light, "Spitfire") seeded by the Ti-Sapphire laser generates 1-mJ energy, 200-fs short pulses at 1-kHz repetition rate. The measured "M^2" parameter of the laser beam profile is $M^2 = 1.8 \pm 0.2$ [27]. The laser energy in the specimen can be precisely varied using two attenuators. Each attenuator involves an electronically controlled rotating half-wave plate that rotates the polarization of the laser beam and a cube beam splitter, where the intensity of the transmitted light depends on its polarization. A fast mechanical shutter is used to select the desired number of pulses for the ablation experiments. The laser beam is tightly focused on the target through an oil-immersion high numerical aperture objective lens (Zeiss $64\times, \mathrm{NA} = 1.4$). The fluorescence imaging system consists of a mercury lamp and an FITC filter set. The excitation filter and the emission filter transmit wavelength ranges of 460–500 nm and 510–560 nm, respectively. The dichroic mirror reflects wavelengths smaller than 510 nm. A cold mirror is used to transmit the laser beam but reflect the fluorescence emission toward either an intensified camera (Roper Scientific, "PI-Max") for two-photon imaging or an interline transfer CCD camera (Princeton Instruments, "Micromax") for epifluorescence imaging. The resulting emission from the focal spot is collected by the tube lens and detected by the CCD camera (6.5 μm pixel size and 2×2 binning). A filter blocks the scattered laser light. A camera exposure time of 300–600 ms is used. Simultaneously with laser axotomy, the system can also perform two-photon imaging with a pair of piezo-driven mirrors that scan the laser beam. A relay-lens system with a pair of lenses (focal lengths of 75 and 160 mm) are used to image the center of the scanning mirrors to the back aperture of the objective lens, to prevent laser beam displacement during scanning. This relay-lens system also enlarges the laser beam to fill the back aperture of the objective lens to achieve diffraction-limited focusing. For the

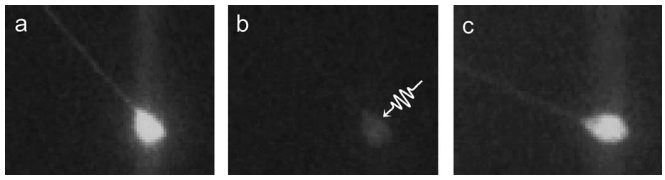

Fig. 3. Recovery from complete photobleaching of a mec-7::GFP-labeled ALMR touch-neuron of an L4 stage worm. (a) Before photobleaching. (b) Five minutes after photobleaching with 1-nJ energy 200-fs short pulses. (c) Three hours after the neuron is completely photobleached. The neuron recovers GFP fluorescence. The same brightness/contrast are used in the images for comparison. The tail of the worm is toward the right bottom corner of the image.

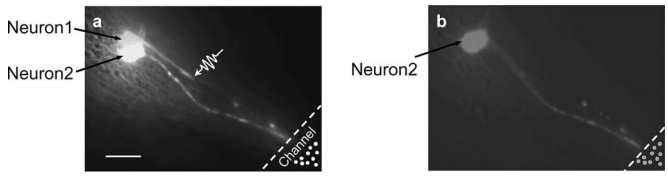

Fig. 4. Axotomy of PHAR phasmid neurons. Prior to axotomy, the worms were incubated in DiO-green dye, and the two nearby neurons could uptake the dye from the channel. After axotomy of the dendrite of one of the neurons, the worms were incubated in DiI-red dye. (a) Under FITC (green) optical filter, both the neurons are visible. (b) Under red optical filter, while the second neuron is visible, the first neuron, whose dendrite was cut, is no longer visible indicating that its dendrite is physically disconnected and it cannot update dyes from the channel following axotomy. The scale bar is 5 μm. The arrow indicates the axotomized part of the dendrite. The tail of the worm is toward the right bottom corner of the image.

experiments reported here, the fluorescence imaging has been sufficient.

IV. Photodamage Threshold: Time-Lapse GFP Fluorescence Photobleaching and Recovery

To determine the energy threshold of cellular photodamage, we have performed controlled photobleaching experiments by exposing cell bodies to laser pulses with different pulse energies at a 1.0-kHz repetition rate. We have completely photobleached the fluorescent signal of GFP-labeled touch and motor neurons. We observed that the fluorescence signal could recover within 3 h after complete photobleaching with pulse energies of 1–2 nJ or lower (Fig. 3). The duration of recovery is consistent with the values reported in the previous photobleaching studies using Argon ion laser-based confocal microscopy [28], which show that the completely photobleached neurons are able to synthesize and recover GFP fluorescence within 3 h. Furthermore, immediately after we photobleached all the motor neurons, the movement of the worms were wild-type (motor neurons are discussed in Section VI). In the regime of the pulse energies (10–40 nJ) we used in axotomy (Section VI), the neurons never recover GFP fluorescence even after 6 h, indicating that a permanent damage occurs instead of simple photobleaching. The worms also cannot move backward (Section VI).

Furthermore, during photobleaching without permanent damage, the entire neuron loses its fluorescence intensity gradually instead of the local laser spot that is being photobleached. This indicates that GFP molecules rapidly diffuse in and out of the photobleached spot, and that it is not possible to have a local photobleached region without photodamage. This is also another indication that the local gap observed after axotomy is not simply due to photobleaching.

V. Dye-Filling Studies to Confirm Axotomy, Target Specificity, and Damage Extent

To test whether the observed loss of GFP signal in the operated axons represents a real lesion, we have conducted dye-filling experiments on phasmid neurons.

The phasmid neurons in *C. elegans* are chemosensory cells located in the tail of the worms. These neurons can be labeled with fluorescent dyes absorbed by their dendrite endings that are exposed to outside through a channel at the tail of the worm. The phasmid neurons were first filled with green fluorescent DiO dye by incubating the worms in the dye solution. Then, we cut the dendrite of a neuron that connects the cell body to the sensory ending. Next, we incubated the worm with red fluorescent DiI dye to test the dye uptake through dendrite following axotomy. The unoperated neuron was completely filled with DiI-red fluorescent dye. In the operated neuron, only the distal part of the laser-operated dendrite took the dye, while the rest of the neuron kept its green label (Fig. 4). These findings indicate a physical disconnection of the dendrites following the laser operation.

The morphology of phasmid neurons provided an opportunity to test the resolution of the laser-assisted axotomy. We were able to cut one of the closely fasciculated dendrites (only few micrometers apart) while leaving the other dendrites intact (Fig. 4). This shows that not only the damage extent is less than a few micrometers, but we can also selectively cut individual nerve processes.

The assessment of damage and the resulting response of the tissue after laser operation are important for understanding tissue permissivity factors on nerve regeneration. Topologically, the motor neuron processes traverse muscle cell membranes that are less than 100 nm away. To assess the extent of the peripheral photodamage (including both vaporization and photobleaching) and the resulting axon retraction, we used a strain where both nerve processes and muscle cell membranes that were in close proximity to the axons were labeled by GFP. We severed the GFP-labeled axons with varying pulse energies and measured the ensuing surrounding damage by loss of GFP signal in the lesion periphery. The observed damaged (dark) region consists of a central region where the tissue is actually removed (ablated/evaporated) and a peripheral region where GFP is photobleached. Fig. 5 shows fluorescence images of axons and their surrounding muscles after axotomy with three different pulse energies (20, 40, and 60 nJ).

From the morphology of fluorescence signal in Fig. 5, we can differentiate the damaged and retracted region of the axons from the photobleached regions: As mentioned in Section IV, the entire body of the neuron loses GFP signal during photobleaching without photodamage. This occurs because GFP molecules are free to diffuse in the cytoplasm. Unless damage occurs, any locally photobleached region rapidly gains GFP signal due to fast

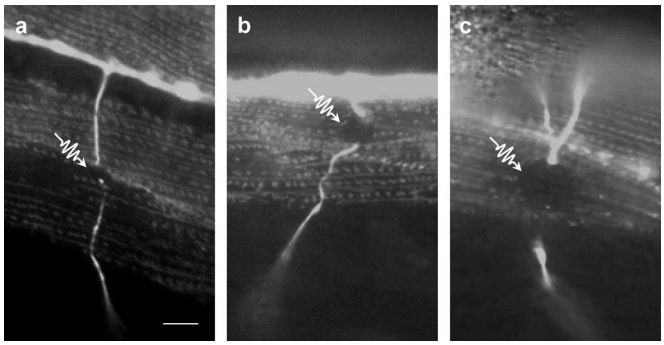

Fig. 5. Fluorescent images of unc-25::GFP axons of the D-type motor neurons and nearby muscle filaments following axotomy and axon retraction after (a) 20-nJ, (b) 40-nJ, and (c) 60-nJ pulse energies at 1-kHz repetition rate with 200-fs short pulses. The GFP-labeled muscle filaments are in less than 100-nm proximity to the GFP-labeled axons. The darker regions are a combination of both photobleached and damaged areas, including retraction of the axons. With increasing pulse energy, the damaged/retracted region of the axon increases rapidly. The scale bar is 10 μm.

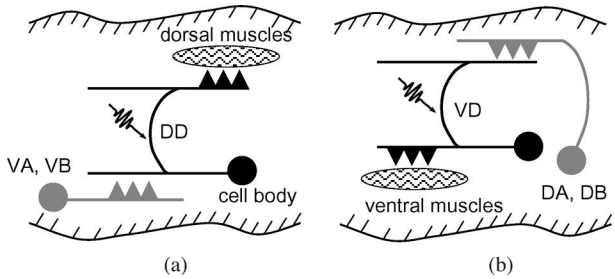

Fig. 6. Synaptic input and output of GABAergic D-type motor neurons. Synaptic connections, neuron cell bodies, and muscles are represented by filled triangles, circles, and dashed ovals, respectively. DD and VD neurons make inhibitory synaptic contacts that control dorsal and ventral muscles, respectively. Their cell bodies are located in the ventral cord of the worm. DD neurons receive cholinergic input from VA and VB neurons. VA and VB neurons also innervate ventral muscles (not shown in the figure). Similarly, cholinergic DA and DB neurons innervate VD neurons (and dorsal muscles that are not shown) in the dorsal side. We cut the D-type neuron processes (indicated by the pulse arrows) that extend from the ventral cord to the dorsal side.

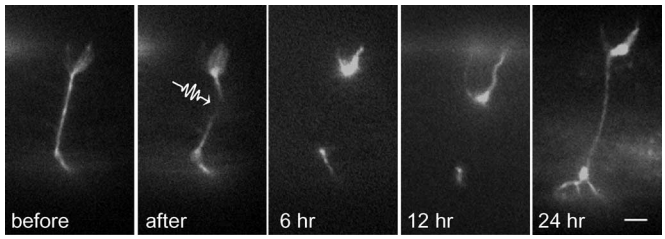

Fig. 7. Nerve regeneration after femtosecond laser axotomy in live *C. elegans*. One hundred pulses with 40-nJ energy and 200-fs short duration at 1-kHz repetition rate are used. Fluorescence images of unc-25::GFP-labeled axons before, after, and following axotomy are shown. Immediately after the axotomy, the worm moved reflexively as seen in the second image. The ventral side of the worm is toward the top edge of the image. The scale bar is 5 μm.

diffusion of the fluorescent GFP molecules from the unbleached regions of the neuron. Thus, in Fig. 5, the regions of axons that have lost GFP signal are actually damaged and retracted where no GFP signal recovery occurs. However, we emphasize that the apparent damage is actually a combination of both ablation and rapid retraction/resealing of the axon following axotomy. In Fig. 5(c) (at the highest energy used, i.e., 60 nJ), the axon retraction is most clearly visible where the axon has retracted a distance larger than the boundary of the photodamaged muscle markers.

The total extent of the photodamage and the following axon retraction increases rapidly with pulse energy. This is in contrast to what happens in the ablation of solid surfaces, where an increase in pulse energy leads to smaller increases in the damaged volume [27]. This may be attributed to the different mechanisms involved in the ablation of biological media [12]. For pulse energies larger than 80 nJ, some worms no longer survive following ablation. These observations indicate the necessity to use sufficiently low pulse energies to reduce the extent of photodamage to the surroundings, in laser surgery of tissues.

VI. Regeneration of Motor Neurons

A. Axon Regrowth

We chose the DD- and VD-type motor neurons in L4-stage worms as targets for laser surgery. Their role in backward locomotion of the worms gives significant advantage in the behavioral assessment of nerve cutting and that following regeneration (Section VI-B). The distinctive morphology of D neurons allows them to receive and provide input on both the ventral and dorsal sides of the body (Fig. 6). Their cell bodies are located in the ventral cord, and they extend circumferential axons toward the dorsal side where they form synapses to body muscles [29] (Fig. 6). These extensions provide favorable targets for laser axotomy.

For axotomy and the following fluorescence imaging of axons, the worms are anesthetized for short periods (15 min) on agarose pads with 5 μL phenoxypropanol per 1 mL agarose. The worms are maintained on standard NGM agar plates at 20 °C.

We cut the circumferential axons (labeled with GFP [30]) at their midbody positions, leaving the rest of the axons intact (Figs. 6 and 7). Both ends of the severed axons initially retract as shown in Fig. 7 at 6 h following axotomy. The axon regrows at 12 h postaxotomy and reaches the dorsal side by 24 h.

For the 10–40-nJ energies we use for axotomy, we also observe cases where aberrant growth or no regrowth occurs (Fig. 8), which is also suggestive of successful axotomy. If our observations were simply photobleaching, no aberrant growth should have been observed. In fact, operated axons mostly show a "de tour" extension, where the regrowing axons do not follow the preaxotomy trajectories.

Among the 52 operated axons (in 11 worms), 54% regrew toward their distal ends within 12–24 h (Fig. 9). Axons that showed partial, aberrant, or no regrowth within 24 h, did not show further improvement for longer observation times (up to 36 h).

B. Functional Recovery: Behavioral Tests

In nerve regeneration studies, the major focus is on the assessment of behavioral recovery. To evaluate functional recovery, we

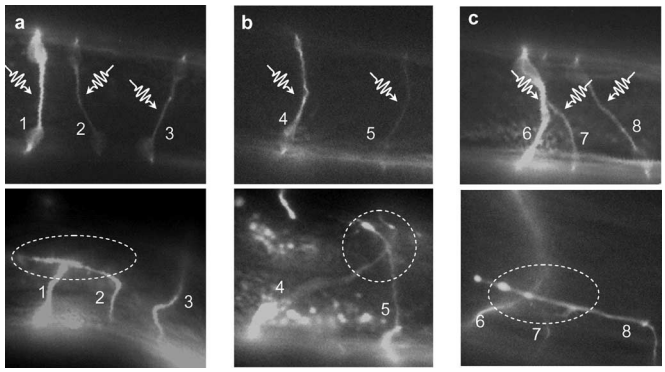

Fig. 8. Three examples of aberrated axon growth cases of the D-type motor neurons. The top panels show stages before axotomy, and the bottom panels show stages 24 h following axotomy. All the axons are ablated at their midbody positions. Ventral side of the worm is toward the bottom side of the images.

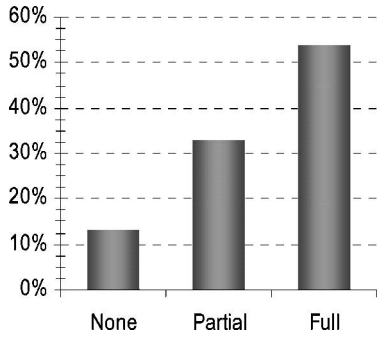

Fig. 9. Statistics of axon recovery after 24 h following axotomy based on the morphology of fluorescence images. A total of 52 axons are followed. The worms are maintained on standard NGM agar plates at 20 °C. One hundred pulses with 40-nJ energy and 200-fs short duration at 1-kHz repetition rate are used.

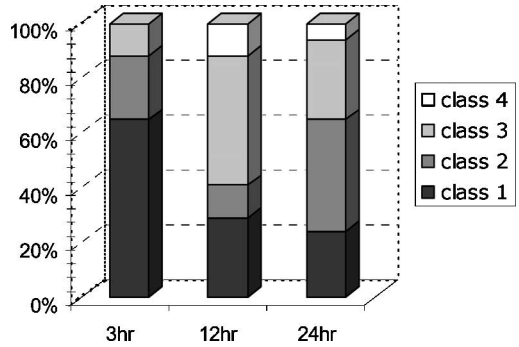

Fig. 10. Time-course analysis of backward motion following axotomy. A total of 17 worms are scored blindly at certain time points using criteria based on the number of backward waves upon each touch to the head, presence or absence of spontaneous backward movement, and deviation from wild-type sinusoidal movement. Improvement in backward motion is graded from complete backward motion deficiency (black) to wild-type (white) in four scores. Sham-operated animals (six in total) show wild-type behavior. Fifteen axons are cut per worm. The worms are maintained on standard NGM agar plates at 20 °C. One hundred pulses with 40-nJ energy and 200-fs short duration at 1-kHz repetition rate are used.

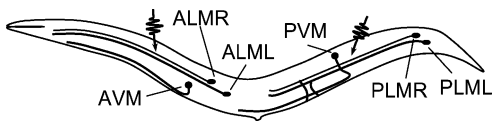

Fig. 11. Touch neurons PLML/R and ALML/R (L, left; R, right) extend processes along the anterior and posterior half of the worm and contribute to mechanosensation in these regions. The cell bodies are shown as black dots. Femtosecond laser axotomy is performed at approximately midpositions of the axons, indicated by the pulse arrows. The other touch neurons AVM and PVM are also shown, which were not operated.

monitored the body motion of the operated worms related to the motor neuron function. Loss of D-neuron function results in simultaneous contraction of the dorsal and the ventral body, which prevents backward motion ("shrinker" phenotype) [31]. We observed a similar loss of function in the worms whose D-neuron nerve processes were severed by laser axotomy.

We scored backward motions of the axotomized and the sham-operated worms from video recordings. Sham-operated control worms were subject to the same axotomy procedure, but the laser beam was focused 5–10 μm away from the target axons. We used criteria such as, the number of backward waves upon each touch to the head, the presence or absence of spontaneous backward movement, and the deviation from wild-type sinusoidal movement. Each movie was given a general score by indexing the subscores of number, pattern, and spontaneity of backward movements. All the movies were scored blindly for condition, i.e., test and control, and time, i.e., randomized time points. The scorings were always consistent when repeated in a different time order and scheme. Worms were recorded at (or around) 3, 12, 24, 36, 48, 54, and 60 h after surgery. Six worms were sham-operated and showed wild-type behavior. Seventeen worms were axotomized and scored as follows.

1) *Score 1:* No backward movement; animal shows defective backward motion.
2) *Score 2:* Animal can move back up to two waves by using irregular muscle contractions instead of smooth sinusoidal ones.
3) *Score 3:* Animal can move backward more than two waves by using irregular muscle contractions instead of smooth sinusoidal ones.
4) *Score 4:* Animal can move backward four or more waves by using sinusoidal muscle contractions—wild-type (WT) behavior.

Operated worms (17 in total, 15 axons per worm) showed the expected "shrinker" phenotype [31] after axotomy, and could not move backward. The sham-operated worms had wild-type movement. Remarkably, the locomotion of operated worms improved toward the wild-type within 12 h (Fig. 10), suggesting that the regenerated axons were functional. As a control, when we ablated neuron cell bodies rather than the neuron processes, worms showed no recovery even after 48 h (data not shown). The correlation of axonal regrowth with behavioral recovery indicates the presence of nerve regeneration in *C. elegans.*

At 24 h postaxotomy, although some worms showed improvement, others showed degradation in locomotion with respect to the 12-h condition (Fig. 8). This could be due to the delay in the establishment of aberrant connections: Our morphological observations using GFP show that proper nerve connections occur mostly within 12 h, whereas it usually takes up to 24 h for aberrantly growing processes to make improper connections. Establishment of these aberrant connections (Fig. 8) can disturb

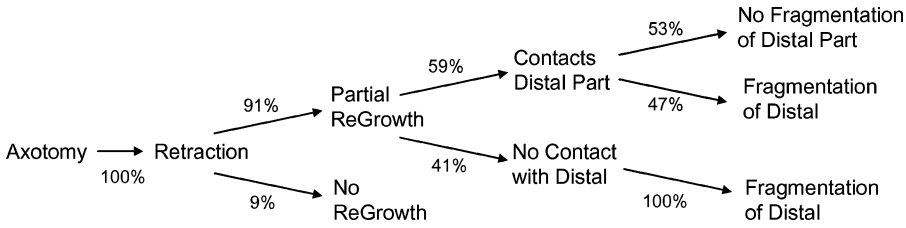

Fig. 12. Degeneration and regeneration pathways of touch neuron processes. Axotomy at midbody of axons of ALM and PLM neurons performed with 200-fs short 100 pulses at 20-nJ energy and 1-kHz repetition rate. A total of 32 neurons (16 ALM and 16 PLM) were followed in 16 worms after axotomy. No statistically significant difference in degeneration or regeneration rates is found between the ALM and PLM neurons. All the neurons exhibited axon retraction within 6 h following axotomy. Ninety-one percent of the neurons showed partial regrowth within 6–24 h. Among 41% of the partially growing neurons, the regrowing axons did not reach their distal parts, and the distal parts went through fragmentation. In the remaining 59% of neurons, the regrowing axons reached distal parts within 24 h following axotomy; among 53% of these cases, the fragmentation of the distal end stopped (followed up to 60 h).

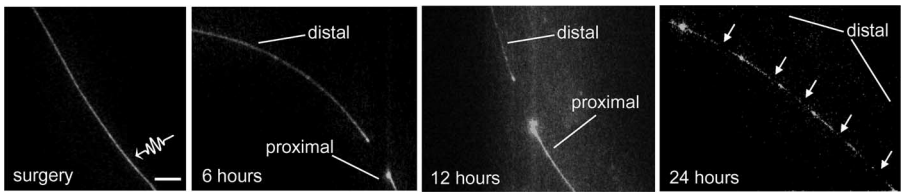

Fig. 13. Axon of a mec-7::GFP-labeled ALMR neuron is shown prior to 6, 12, and 24 h following axotomy. Cell body is not shown. Twelve hours after axotomy, the proximal end did not regrow, and the distal end showed weak GFP fluorescence. Twenty-four hours after axotomy, the distal part of the axon showed fragmented GFP fluorescence. The scale bar is 10 μm.

the sinusoidal waves in worm motion, and thus could be responsible from the slight degradation in locomotion at 24 h following the major improvement observed at 12 h (Fig. 10).

A supplementary movie[1] shows the behavioral response of an axotomized worm. The movie includes two parts. Part I shows an axotomized worm 3 h after the axotomy. The worm can move forward like the wild-type. When we touch its head, it attempts to move backward but it cannot move; instead its body segments shrink. Part II shows the same worm 24 h after the axotomy, and it is able to move backward with sinusoidal body motions when we touch its head.

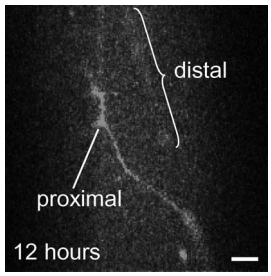

Fig. 14. Axon of an ALMR neuron is shown 12 h following axotomy. Cell body is not shown. The proximal end regrew astray, and the GFP fluorescence of the distal part became vanishingly small. The scale bar is 10 μm.

VII. Regeneration of the Touch Neurons

Different neuron types have differential capacities for recovery after nerve injury, probably regulated by permissivity factors in the tissue environment and the intrinsic qualities of neurons. We established a nerve injury technique involving GABAergic motor neurons of *C. elegans* in the previous sections. In this section, we report our studies of axotomy in touch neurons that form the components of mechanosensory neural circuit in the worm: PLM and ALM neurons contribute to the sensation of soft touch in the anterior and posterior half of the animal (Fig. 11) [32]. They transduce mechanical stimuli from the outside world to the nervous system. Their distinctive morphology and cellular character provide a venue to investigate not only the differential neuronal response to injury but also the interaction of severed axon ends after laser-assisted axotomy.

We conducted axotomy on 16 ALM and 16 PLM neurons at the midbody locations of their axons in 16 worms (200-fs short 100 pulses with 20-nJ energy at 1-kHz rate). We observed the severed axons at 6, 12, 24, and 60 h following axotomy, and found no statistically significant difference in the regeneration and degeneration behaviors between the ALM and PLM neurons. Fig. 12 shows our findings.

All operated axons showed retraction of the two severed ends, seen as a blobby shape following axotomy. Ninety-one percent of the axons showed partial regrowth from the proximal ends within 6–24 h; the distal ends did not show any sign of regrowth. Among the regrowing axons, 41% did not reach the cut distal counterpart; and in these cases, the distal axons all showed fragmented GFP fluorescence (Figs. 13 and 14), a sign we interpret as degeneration. In the remaining 59% of the neurons, the proximal axons regrew in a trajectory that follows closely the original axons and reached the distal ends within 24 h. In 53% of these regenerating neurons, the distal ends did not show any sign of fragmentation in GFP fluorescence (followed up to 60 h) (Fig. 15). As we did not perform axotomy on all touch neurons in a given animal, we were not able to assay touch response to assess whether salvage of distal part of the axon from fragmentation caused complete recovery of the injured axons.

[1][Online]. Available: http://www.rle.mit.edu/yanik/regeneration.mov

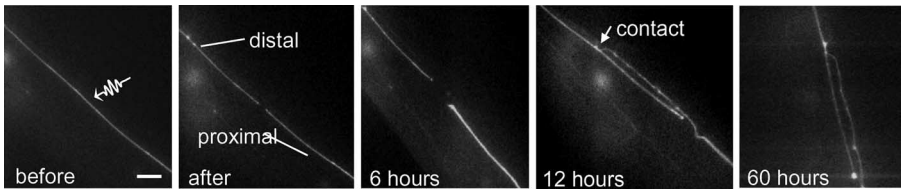

Fig. 15. Axon of an ALMR neuron is shown prior to, afterward, and 6 and 12 h following axotomy. Cell body is not shown. Six hours after axotomy, retraction of the proximal end of the axon is seen. Twelve hours after axotomy, the regrowing proximal part of the axotomized axon reached and bypassed the laser operation point, and made close contact with the distal part. No fragmentation of the distal part of the axon is seen even after 60 h following axotomy. The scale bar is 10 μm.

It is worth noting that the distal ends of the motor neurons also did not fragment for at least 24 h following retraction. However, since regrowth of the motor neuron processes was quite fast and reached the dorsal cord, it was not possible to observe whether the injured distal end of motor neurons underwent fragmentation or the regrowing proximal part made direct contact to the distal severed counterpart. On the other hand, in touch neurons, we could clearly distinguish the injured distal ends from the newly but somewhat slowly growing proximal ends of the axons.

Recovery of the distal ends of the injured axons can occur in leech through axon fusion [33] or through other mechanisms such as gap-junction formation [34]. In *C. elegans*, further studies are required to analyze the cellular interactions between the growing proximal axon ends and the distal ends.

Different neuronal processes have different regeneration capacities determined by both intrinsic and extrinsic factors. The dendrites of phasmid neurons did not display any regeneration following axotomy in our experiments (Section V). In contrast, we observed regeneration in both the DD/VD motor neurons and the ALM/PLM touch neurons (Sections VI and VII): The ALM and PLM touch neuron processes are axonal. On the other hand, the VD and DD motor neurons display a mixture of both dendritic and axonal characteristics, where axonal properties are more dominant in the DD neurons than in the VD neurons. We did not observe a significant difference between the regeneration capacities of VD and DD motor neuron processes, which could be due to the fact that both DD and VD processes respond to similar guiding cues.

VIII. Concluding Remarks

Femtosecond laser axotomy is a novel technique that can be performed with high repeatability with submicrometer precision and high speed. It takes less than a minute to find, position, focus, and cut an axon. Including the time to prepare slides, anesthetize the worms, cut 15 D-type axons, and recover the axotomized worms, the entire process is completed within 10 min per worm. We found that with 10–40-nJ pulse energies and with only 100 pulses, we can focus the laser on the target easily and perform axotomy rapidly without any misses.

The use of femtosecond laser pulses as a precise surgical tool allowed us, for the first time, to observe and study nerve regeneration in *C. elegans* that has a simple nervous system. Since simple organisms like *C. elegans* provide tremendous research potential due to their amenable genetics and screening methods, application of femtosecond laser axotomy technique should allow rapid screening of genes and molecules affecting nerve regeneration and development.

Acknowledgment

The authors would like to thank Prof. R. Byer of Stanford University for allowing the experiments to be performed at his laboratories. M. F. Yanik and A. Ben-Yakar would like to thank Prof. S. Fan and Prof. R. Byer, for their support. The authors would also like to thank Prof. M. Fejer, Prof. J. Santiago, Prof. M. G. Mungal, Prof. O. Solgaard, Prof. D. Palanker, Dr. E. Kolby, and Prof. K. Shen of Stanford University for lending valuable research equipment.

References

[1] P. J. Horner and F. H. Gage, "Regenerating the damaged central nervous system," *Nature*, vol. 407, pp. 963–970, 2000.
[2] D. H. Bhatt, S. J. Otto, B. Depoister, and J. R. Fetcho, "Cyclic AMP-induced repair of Zebrafish spinal circuits," *Science*, vol. 305, pp. 254–258, 2004.
[3] M. F. Yanik, H. Cinar, H. N. Cinar, A. Chisholm, Y. Jin, and A. Ben-Yakar, "Neurosurgery: Functional regeneration after laser axotomy," *Nature*, vol. 432, p. 822, 2004.
[4] R. L. Amy and R. Storb, "Selective mitochondrial damage by a ruby laser microbeam: An electron microscope study," *Science*, vol. 150, pp. 756–757, 1965.
[5] M. W. Berns *et al.*, "Laser microsurgery in cell and developmental biology," *Science*, vol. 213, pp. 505–513, 1981.
[6] M. W. Berns, W. H. Write, and R. W. Steubing, "Laser microbeam as a tool in cell biology," *Int. Rev. Cytol.*, vol. 129, pp. 1–44, 1991.
[7] C. R. Cowan and A. A. Hyman, "Centrosomes direct cell polarity independently of microtubule assembly in *C. elegans* embryos," *Nature*, vol. 431, pp. 92–96, 2004.
[8] S. W. Grill, J. Howard, E. Schäffer, E. H. K. Stelzer, and A. A. Hyman, "The distribution of active force generators controls mitotic spindle position," *Science*, vol. 301, pp. 518–521, 2005.
[9] M. R. Samoiloff, "Nematode morphogenesis: Localization of controlling regions by laser micro-beam surgery," *Science*, vol. 180, p. 976, 1973.
[10] A. Khodjakov, S. La Terra, and F. Chang, "Laser microsurgery in fission yeast: Role of the mitotic spindle midzone in anaphase B," *Curr. Biol.*, vol. 14, p. 1330, 2004.
[11] A. A. Oraevsky, L. B. Da Silva, A. M. Rubenchik, M. D. Feit, M. E. Glinsky, M. D. Perry, B. M. Mammini, W. Small IV, and B. C. Stuart, "Plasma mediated ablation of biological tissues with nanosecond-to-femtosecond laser pulses: Relative role of linear and nonlinear absorption," *IEEE J. Sel. Topics Quantum Electron.*, vol. 2, no. 4, pp. 801–809, Dec. 1996.
[12] A. Vogel, J. Noack, G. Huttman, and G. Paltauf, "Mechanisms of femtosecond laser nanosurgery of cells and tissues," *Appl. Phys. B*, vol. 81, p. 1015, 2005.
[13] M. D. Perry *et al.*, "Ultrashort-pulsed laser micromachining of dielectric materials," *J. Appl. Phys.*, vol. 85, pp. 6803–6810, 1999.
[14] A. Vogel *et al.*, "Energy balance of optical breakdown at nanosecond and femtosecond time scales," *Appl. Phys. B*, vol. 68, pp. 271–280, 1999.
[15] K. König, I. Riemann, P. Fischer, and K. Halbhuber, "Intracellular nanosurgery with near infrared femtosecond laser pulses," *Cell. Mol. Biol.*, vol. 45, p. 195, 1999.

[16] E. L. Botvinick, V. Venugopalan, J. V. Shah, L. H. Liaw, and M. W. Berns, "Controlled ablation of microtubules using a picosecond laser," *Biophys. J.*, vol. 87, p. 4203, 2004.
[17] W. Watanabe, N. Arakawa, S. Matsunaga, T. Higashi, K. Fukui, K. Isobe, and K. Itoh, "Femtosecond laser disruption of subcellular organelles in a living cell," *Opt. Express*, vol. 12, pp. 4203–4213, 2004.
[18] I. Tolic, L. Sacconi, G. Thon, and F. Pavone, "Positioning and elongation of the fission yeast spindle by microtubule-based pushing," *Curr. Biol.*, vol. 14, p. 1181, 2004.
[19] N. Shen, D. Datta, C. B. Schaffer, P. LeDuc, D. E. Ingber, and E. Mazur, "Ablation of cytoskeletal filaments and mitochondria in cells using a femtosecond laser nanoscissor," *Mech. Chem. Biosyst.*, vol. 2, p. 17, 2005.
[20] J. Colombelli, E. G. Reynaud, J. Rietdorf, R. Pepperkork, and E. H. K. Stelzer, "In vivo selective cytoskeleton dynamics quantification in interphase cells induced by pulsed ultraviolet laser nanosurgery," *Traffic*, vol. 6, p. 1093, 2005.
[21] K. Konig, W. Riemann, and W. Fritzsche, "Nanodissection of human chromosomes with near-infrared femtosecond laser pulses," *Opt. Lett.*, vol. 26, pp. 819–821, 2001.
[22] U. K. Tirlapur and K. König, "Targetted transfection by femtosecond laser," *Nature*, vol. 418, pp. 290–291, 2002.
[23] W. Supatto, D. Debarre, B. Moulia, E. Brouzes, J. L. Martin, E. Farge, and E. Beaurepaire, "In vivo modulation of morphogenetic movements in Drosophila embryos with femtosecond laser pulses," *Proc. Nat. Acad. Sci.*, vol. 102, p. 1047, 2005.
[24] N. Nishimura, C. B. Schaffer, B. Friedman, P. S. Tsai, P. D. Lyden, and D. Kleinfeld, "Targeted insult to subsurface cortical blood vessels using ultrashort laser pulses: Three models of stroke," *Nature Methods*, vol. 3, p. 99, 2006.
[25] W. Denk, J. H. Strickler, and W. W. Webb, "Two-photon laser scanning fluorescence microscopy," *Science*, vol. 248, pp. 73–76, 1990.
[26] J. Colombelli, S. W. Grill, and E. H. K. Stelzer, "UV diffraction limited nanosurgery of live biological tissues," *Rev. Sci. Instrum.*, vol. 75, pp. 472–478, 2004.
[27] A. Ben-Yakar and R. L. Byer, "Femtosecond laser ablation properties of borosilicate glass," *J. Appl. Phys.*, vol. 96, no. 9, p. 5316, 2004.
[28] N. D. Dwyer *et al.*, "Polarized dendritic transport and the AP-1 mu1 clathrin adaptor UNC-101 localize odorant receptors to olfactory cilia," *Neuron*, vol. 31, pp. 277–287, 2001.
[29] J. G. White, E. Southgate, J. N. Thomson, and S. Brenner, "The structure of the nervous system of the nematode *Caenorhabditis elegans*," *Philos. Trans. R. Soc. Lond. B, Biol. Sci.*, vol. 314, pp. 1–340, 1986.
[30] X. Huang, H. J. Cheng, M. Tessier-Lavigne, and Y. Jin, "MAX-1, a novel PH/MyTH4/FERM domain cytoplasmic protein implicated in netrin-mediated axon repulsion," *Neuron*, vol. 34, pp. 563–576, 2002.
[31] S. L. McIntire, E. Jorgensen, J. Kaplan, and H. R. Horvitz, "The GABAergic nervous system of *Caenorhabditis elegans*," *Nature*, vol. 364, pp. 337–341, 1993.
[32] M. Chalfie, "The differentiation and function of the touch receptor neurons of *Caenorhabditis elegans*," *Prog. Brain Res.*, vol. 105, pp. 179–82, 1995.
[33] S. A. Deriemer, E. J. Elliott, E. R. Macagno, and K. J. Muller, "Morphological evidence that regenerating axons can fuse with severed axon segments," *Brain Res.*, vol. 272, pp. 157–61, 1983.
[34] J. M. Camhi and E. Macagno, "Using fluorescence photoablation to study the regeneration of singly cut leech axons," *J. Neurobiol.*, vol. 22, no. 2, pp. 116–129, 1991.

Mehmet Fatih Yanik received the B.S. and M.S. degrees in electrical engineering and physics from the Massachusetts Institute of Technology (MIT), Cambridge, in 2000. He received the Ph.D. degree in applied physics from Stanford University, Stanford, CA, in 2005.

He briefly worked in the area of quantum computing at Xerox Parc, Palo Alto, CA, and in the area of molecular electronics at HP Labs, Palo Alto, CA, with Stanley Williams, and most recently on single molecule imaging in microfluidics with Steve Quake at Stanford Bioengineering. Currently, he is an Assistant Professor of Electrical Engineering at MIT and a Faculty Member of the MIT Computational and Systems Biology Program. He is also associated with the Ginzton Laboratory, Stanford University. His research interests include femtosecond laser nanosurgery, micro and nanomanipulation, nerve regeneration and degeneration, subdiffraction limit imaging, and nanophotonic devices.

Dr. Yanik's thesis work with Rajeev Ram on˜ultrafast spin spectroscopy received the MIT-Chorafas Best Thesis Award.˜He invented the all-optical coherent photon storage, which was selected among the top ten research advances of the year by the *Technology Research News Magazine* in 2004. His work on nanophotonic devices was awarded first place in the 2004 Innovator's Challenge Competition in Silicon Valley. He has been selected the "The Outstanding Young Person" by Junior Chamber International's Branch in 2004.

Hulusi Cinar received the M.D. degree, in 1990 and the Specialist degree in medical physiology, in 1994 from Ege University School of Medicine, Turkey, and Dokuz Eylul University School of Medicine, Turkey, respectively. He received the Ph.D. degree in neuroscience in 2001 from Baylor College of Medicine, Houston, TX.

Since 2002, he has been with the University of California, Santa Cruz, as a member of the postgraduate staff. His research has been concerned with the motor nervous system of *C. elegans*, a genetic model organism. His current research interests include nerve regeneration, neuron-specific genomics, neuronal circuits, and modeling of motor behavior.

Hediye Nese Cinar received the M.D. and the Specialist in Medical Physiology degrees from Dokuz Eylul University School of Medicine, Turkey, in 1987 and 1994, respectively.

After moving to the United States, she worked on brain injury and disease models. In 1997, she joined Baylor College of Medicine, Houston, TX, for research on the organogenesis in *C. elegans* using uterus development as a model system. Since 2002, she has been working on morphogenesis and head formation of *C. elegans* at the University of California, Santa Cruz. Her current research interests include morphogenesis, organ formation, and nerve regeneration.

Aaron Gibby received the B.S. degree in materials science and engineering from Cornell University, Ithaca, NY, in 1999, and the M.S. degree in electrical engineering from Stanford University, Stanford, CA, in 2005. He is currently working toward the Ph.D. degree at Stanford University in novel nonvolatile memory applications.

Andrew D. Chisholm received the B.A. degree from Clare College, Cambridge University, Cambridge, U.K., in 1986. He received the Ph.D. degree from the U.K. Medical Research Council Laboratory for Molecular Biology, Cambridge, in 1990.

Currently, he is a Professor of Molecular, Cell and Developmental Biology in the Department of Biology, University of California, Santa Cruz.

Yishi Jin received the B.Sc. degree (Hons.) in cell biology from Peking University, Beijing, China, in 1984, and the Ph.D. degree in molecular biology from the University of California, Berkeley, in 1991.

After postdoctoral work at Massachusetts Institute of Technology, Cambridge, she became an Assistant Professor of Biology at the University of California, Santa Cruz, in 1996. She is currently a Professor of Biology, and an Investigator with the Howard Hughes Medical Institute, Chevy Chase, MD. Her current research interests include understanding the molecular mechanism of neuronal wiring.

Adela Ben-Yakar received the B.Sc. (*cum laude*) and M.Sc. degrees in aerospace engineering from The Technion—Israel Institute of Technology, Haifa, Israel, in 1992 and 1995, respectively. She received the Ph.D. degree in mechanical engineering from Stanford University, Stanford, CA, in 2000.

During 2000–2004, she was a Postdoctoral Researcher in applied physics at Stanford University and a Visiting Scholar at Harvard University, Cambridge, MA. She is currently an Assistant Professor in the Mechanical Engineering Department at the University of Texas at Austin and a Member of the Graduate Student Council in the Biomedical Engineering Department and Institute of Neurosciences. Her current research interests include femtosecond laser tissue interactions, femtosecond-laser nanosurgery, plasmonic laser nanosurgery, two-photon imaging, and fs-laser applications for diagnosis and treatment of cancer and for *in vivo* nerve regeneration studies.

Prof. Ben-Yakar is a member of the Optical Society of America (OSA) and the International Society for Optical Engineering (SPIE). She was the recipient of the Fulbright Scholarship in 1995, the Zonta Amelia Earhart Award in 1995, and the International Sephardic Education Foundation Scholarship from 1995 to 2000.